Feito, N., Díaz-Álvarez, J., López-Puente, J. & Miguelez, M. (2018). Experimental and numerical analysis of step drill bit performance when drilling woven CFRPs. *Composite Structures, vol. 184*, pp. 1147–1155.

DOI: 10.1016/j.compstruct.2017.10.061

Experimental and numerical analysis of step drill bit performance when drilling woven CFRPs

N. Feito[a,*], J. Díaz-Álvarez[b], J. López-Puente[c], M.H. Miguelez[a]

[a] Department of Mechanical Engineering, Universidad Carlos III de Madrid, Avda. Universidad 30, 28911 Leganés, Madrid, Spain
[b] Department of Bioengineering and Aerospace Engineering, Universidad Carlos III de Madrid, Avda. Universidad 30, 28911 Leganés, Madrid, Spain
[c] Department of Continuum Media and Structural Analysis, Universidad Carlos III de Madrid, Avda. Universidad 30, 28911 Leganés, Madrid, Spain

ARTICLE INFO

Keywords:
Drilling
CFRP
Numerical modelling
Delamination

ABSTRACT

This paper focuses on the influence of the step drill bit geometry on the damage induced during drilling Carbon Fiber Reinforced Polymer materials (CFRPs). Step geometry designed with the aim of avoiding composite damage in CFRPs drilling, is compared to conventional twist configuration. Despite the reduction of thrust force and torque observed when using the step drill, the delamination was only reduced at low feed rates. A numerical model developed for the step geometry was validated with experimental data demonstrating its ability to predict thrust force and delamination for different values of feed rate and cutting speed. Numerical model allowed the development of a parametrical study. Finally, using a response surface methodology a mechanistic model and surface diagrams have been presented in order to help in the selection of optimum variables minimizing drilling induced damage.

1. Introduction

Long Fibre Reinforced Polymers (LFRPs) are widely used in the aerospace industry, mainly those reinforced with carbon fibres (CFRPs) because of their excellent mechanical/physical properties and low weight [1].

Aircraft manufacture involves the production of high value near-net-shape CFRPs components and further mechanical joining using rivets or bolts are required. Despite some intents in implementing new processes to make holes in CFRP materials such as water jet cutting [2,3] or laser machining [4,5], conventional drilling is still the most common machining process in aerospace sector [6,7]. CFRPs are considered low machinability materials due to the abrasive character of the fiber reinforcement causing tool wear and the nature of the material susceptible to experience drilling induced damage, mainly delamination. Workpiece damage induced during machining process can affect the service life of the component [8,9]. Designing new tools with better performance including both cost and damage reduction during drilling is still a challenge for the aerospace industry [10,11].

Drilling induced defects have been analyzed in previous work of the authors [12]. In agreement with other works, it was observed that delamination is the prevalent damage induced in the composite during drilling [13,14]. Delamination generally increases with the feed rate [15] even at high speed [16,17], and it is also enhanced due to tool wear progression [18]. The increase of the feed rate, raises the pull-out force, and consequently, the damaged zone around the hole exit. The wear progression due to the abrasive effect of the fibres modify the cutting geometry of the worn tool leading to thrust force increment and hole quality decrease.

The drill geometry is also a key factor influencing hole quality, not only in composite drilling. For instance, the two-edged angle drill bit improves the process diminishing tensile residual stresses in the steel workpiece [19]. Feito et al. [12] and Karnik et al. [20] observed that delamination increased with the point angle of the twist drill bit for conventional and high speed drilling of woven-ply CFRP laminates. Special designs of drill bits have been tested in different scientific works in order to reduce delamination [21–30]. A brief state of the art summarizing the main contributions is provided below.

Tsao and Hocheng [21,22] compared the performance obtained with three different geometries. The candle stick drill and saw drill caused smaller delamination factor than that obtained with twist drill. The feed rate and drill diameter were the most influencing parameters on the overall performance.

Feito et al. [23] observed that reamer geometry presented low influence of cutting parameters in thrust force. This tool was the most adequate geometry compared to twist drill and step drill bits for drilling woven materials machining at low feed rate and high cutting speed. In agreement with this result, Durao et al. [24] showed that twist and

* Corresponding author.
E-mail address: nfeito@db.uc3m.es (N. Feito).

Received 1 August 2017; Received in revised form 4 October 2017; Accepted 17 October 2017

special step drills did not show considerable changes in delamination when feed rate was increased

Hocheng and Tsao [25,26] carried out drilling analysis on woven CFRPs with large thickness, proved that delamination at the hole exit was reduced using a drill with a small chisel edge; thus, saw and core drills showed better results than step geometry and twist drill.

Shyha et al. [27,28] observed a reduction in the feed force with the use of step geometry [27,28]. This was attributed to the lower interaction between the chisel edge and the workpiece. At the same time, drilling at elevated feed rate reduced the contact time between the cutting tool and workpiece material thus reducing abrasive action. In agreement with these observations Brinksmeier and Janssen [29] concluded that the use of adapted step drills improved diameter tolerances, surface quality, and tool wear. Marques et al. [30] also proved that step geometry reduced the thrust force during drilling decreasing the risk of delamination due to the generation of a pilot hole with the first part of the drill bit.

Drilling is a complex process influenced by multiple factors. Mechanistic models are interesting predictive tools helping in the establishment of the drilling process ensuring safety conditions for the workpiece. Predictive models can be found in the literature for steel materials [19,31], GFRP materials [32,33] and CFRP materials [34–37]. Mechanistic models based on experimental tests established a correlation between the cutting parameters and the thrust force for different geometries (brad-point drill bit, slot drill bit, step drill). A recent work considered alternative layer effect of fibre reinforced plastic composite and tool edge radius effects of micro-drill to predict thrust force and torque [38].

Analytical models have been also developed to calculate the critical thrust force as a function of the different parameters related to the tool geometry. Hocheng & Tsao developed this idea in some studies [24,25] for different geometries: brad point drill bit, slot drill bit, step drill bit, and core drill bit. Critical thrust forces causing the onset of delamination theoretically predicted matched reasonably experimental results. Girot et al. presented a complex orthotropic analytical model able to predict the critical thrust force causing delamination in CFRPs drilling [39]. The more recent models considered mix loads conditions and detailed the thermal effect of the drilling operation [40,41].

Numerical models of drilling based on Finite element method (FEM) were recently developed to predict inter-laminar in composites. Chinmaya et al. [42] recently published a review of machining models of different types of composites. Numerical modeling, once the model is validated, is a powerful tool allowing uncoupling the parameters influencing the drilling process and providing estimation of difficult to measure variables.

Early models modeling the machining of composite materials were focused on orthogonal cutting developing both 2D and 3D approaches [43–45]. These studies analyzed the influence of the fibres orientation or the rounding of the cutting tool for example. However, despite the advantages of this approach focused on orthogonal cutting, this simplification is far from the real industrial processes involving 3D cutting.

Drilling simulation requires 3D modeling. Mainly two approaches have been used in literature: simplified modeling (quasi-static model) and complete modeling simulating chip removal. The first approach considers the drill bit as a punch, and a force or displacement is applied on it. Some authors used this approach to study the damage generated during drilling in GFRPs [32] and CFRPs materials [46,47] as a function of thrust force. Durao et al. [46,47] used the model to analyze the influence of the drill point angle, concluding that sharper tools induce less damage than higher point angles.

The second approach reproduces the rotatory movement and the drill penetration on the workpiece and also the material failure and chip removal [48–50]. This type of model is difficult to implement due to the high computational cost and the complex geometry of the drill bit which has to be reproduced. A comparison between both approaches has proved that, although simplified model overestimates the delamination damage it reduces significantly the computational time due to its simplicity [51]. However detailed analysis of drill geometry should be developed with the realistic complex model considering chip removal.

This paper focuses on the performance of the step drill when drilling CFRPs. This is relatively new geometry that has been poorly analyzed in the literature. The aim is analyzing the performance of this geometry and developing a mechanistic model providing an easy predictive tool suitable even for industrial environment. Numerical model of the drilling process reproducing the step geometry was developed and validated in comparison to experimental results. The model was used to estimate trust force and delamination for different cutting parameters and back supporting conditions in order to feed the mechanistic model. The paper is structured in this brief introduction followed by the description of the experimental work in the second section. Third section presents numerical modeling of drilling process. Once the model was validated a parametrical study was developed adjusting a mechanistic model for prediction of the main variables involved in the process. Finally conclusions of the work are stated in the last section.

2. Experimental work

In this section, the experimental device, including materials, cutting tools and measurement systems used in the drilling tests are described. The aim is analyzing the performance of the stepped geometry when compared to conventional drill. Moreover the experimental results required for further validation of the model are presented.

2.1. Workpiece material and drills

Tests were carried out on plates (120 mm × 29 mm and 2.2 mm thick) composed of 10 layers of woven CFRP based on AS-4 carbon fiber and 8552-epoxy matrix (55.29% resin content) manufactured by Hexcel Composites. The mechanical properties provided by the composite manufacturer for the composite material are shown in Table 1, where E_i is elastic modulus in the direction i; υ_{ij} is the poisson coefficient; G_{ij} is the elastic modulus in shear directions; X_t, Y_t and S_t are the maximum tensile stress in longitudinal and shear directions respectively; Finally, X_c and Y_c are the maximum compressive stress in longitudinal directions.

Two different drill tool geometries manufactured by GUHRING were compared. Main dimensions of drill bits with nominal diameter 6 mm are shown in Fig. 1. The conventional tool has a point angle of 118° (Fig. 1A). The step geometry has a change of section from 4 mm to 6 mm. The length of the step is 6.6 mm (Fig. 1B). Tools are based on CW substrate without coating and were tested in fresh conditions (unworn).

2.2. Drilling tests

Drilling tests were carried out using a machining center (KONDIA B-500). Thrust force during machining was measured using a dynamometer Kistler 9123C. The acquisition system coupled to the machine tool is shown in Fig. 2A.

The cutting parameters for the experimental test are summarized in Table 2. The range was selected following the recommendations of the

Table 1
Mechanical properties of the composite.

Property	Units	Value	Property	Units	Value
ρ	[kg/m^3]	1570	G_{12}	[GPa]	5
$E_1 = E_2$	[GPa]	68	$G_{23} = G_{13}$	[GPa]	1.5
E_3	[GPa]	10	$X_t = Y_t$	[MPa]	795
ν_{12}	–	0.22	$X_c = Y_c$	[MPa]	860
$\nu_{13} = \nu_{23}$	–	0.49	S_t	[MPa]	98

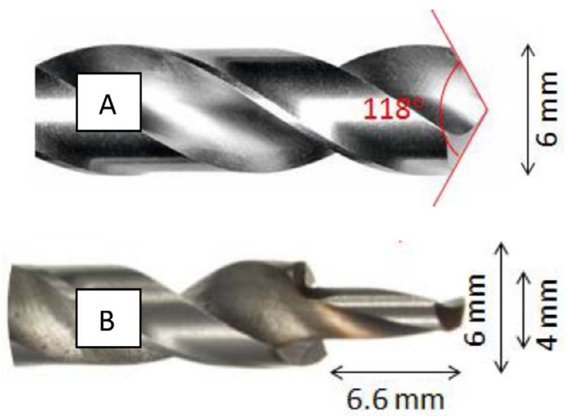

Fig. 1. Main dimensions for both tools testes: twist (A) and step (B).

drills manufacturer GUHRING for drilling CFRPs. At the same time, the drilling experiments were conducted without coolant because it is required to avoid the composite contamination with the cutting fluid.

Damage in the workpiece was quantified in terms of the delamination factor (F_d) defined as the ratio between the maximum diameter of delaminated area and the nominal diameter of the hole (see Fig. 2B). Both diameters were measured through the analysis of optical images of the machined holes obtained with a stereo microscope (Optika SZR).

3. Experimental results

Thrust force and torque for both conventional and step drills, were recorded during the tests and the maximum value obtained during each experiment is presented in Tables 3 and 4. Postmortem analysis of the workpiece allowed obtaining the delamination factor at the hole entry and exit. The measured values are also summarized in Tables 3 and 4.

The evolution of maximum values of thrust force with feed rate is presented in Fig. 3 for the twist drill and the step drill (maximum thrust force during step 1 and 2 were represented). In general, it is observed that the thrust force increases with feed rate, although in the case of Step 2 this trend is almost inappreciable. Spindle speed had an opposite effect, it is observed a slightly decrease of the feed force with cutting speed, but the influence of cutting speed is much lower than the effect of the feed rate. These observations agree with previous studies [24,28] where the trending of the cutting forces are positive with feed fare having this parameter more influence than cutting speed. However these studies do not make difference between the first and the second step in the case of step geometry and use a very limited range of cutting parameters.

Thrust force for step geometry is lower than that obtained with twist tool due to the lower effective diameter machined reaching a decrease of 25% in the first step and 73% in the second step. With this special

Table 2
Range of cutting parameters used in drilling tests.

Parameter	Range		
Cutting speed (m/min)	25	50	100
Feed rate (mm/rev)	0.05	0.1	0.15

Table 3
Experimental data measured during tests for twist geometry.

Cutting speed (m/min)	Feed rate (mm/rev)	Thrust force (N)	Torque (N·mm)	Entry delamination	Exit delamination
25	0.05	53.071	109.9	1.13	1.09
	0.1	64.48	167.84	1.31	1.09
	0.15	94.69	201.21	1.37	1.10
50	0.05	53.9	138.1	1.30	1.08
	0.1	68.24	147.91	1.32	1.08
	0.15	74.38	187.6	1.35	1.14
100	0.05	56.2	156.25	1.20	1.07
	0.1	69.93	167.17	1.21	1.07
	0.15	86.014	177.45	1.23	1.11

geometry, part of the damage generated in the material with the first section is eliminated with the material removed with the second section as it was also reported by Marques et al. [30]. Similar behavior is observed for torque increasing with feed rate and decreasing with cutting speed (Fig. 4). The values of torque for step geometry are lower than those obtained for the case of twist drill bit. Differences for both steps when compared to conventional geometry are 51% for the first step and 74% for the second step.

The delamination factor F_d, calculated as the ratio between maximum diameter of delaminated area and the nominal diameter of the drill (6 mm), is presented in Fig. 5. It is observed that, in general, step geometry reduces the damage especially at the entry hole (between 22 and 25%). The damage at the exit is decreased when low feed rates are selected. This effect was also observed by Durao et al. [24] who only studied the influence of the feed rate at one fixed cutting speed.

4. Numerical model and validation

4.1. Model development

The numerical model was developed in ABAQUS/Explicit code. Both drill geometries (twist and step, shown in Fig. 1) were detailed drawn in CAD software and further imported to ABAQUS/Explicit code. Rotary and feed movements were imposed on the tool it is illustrated in Fig. 6A.

The displacement of the workpiece in Z direction was restricted at

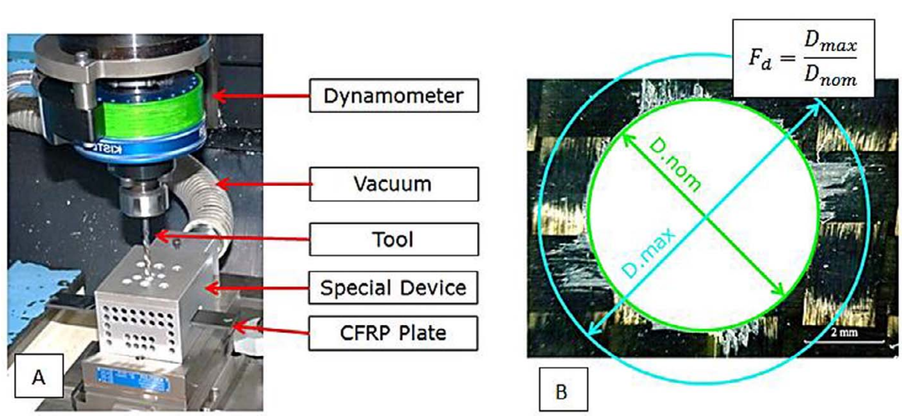

Fig. 2. Experimental device (A) and calculation of delamination factor (B).

Table 4
Experimental data measured during tests for step geometry.

Cutting speed (m/min)	Feed rate (mm/rev)	Thrust force Step 1 (N)	Thrust force Step 2 (N)	Torque Step 1 (N·mm)	Torque Step 2 (N·mm)	Entry delamination	Exit delamination
25	0.05	45.69	21.46	40.36	82.97	1.28	1.07
	0.1	60.72	22.15	79.72	121.47	1.33	1.10
	0.15	78.97	26.47	99.24	145.54	1.34	1.14
50	0.05	62.46	21.45	52.52	83.55	1.33	1.09
	0.1	80.63	21.39	97.9	132.99	1.36	1.15
	0.15	115.65	19.88	113.53	164.01	1.39	1.17
100	0.05	42.29	18.35	41.23	76.17	1.32	1.11
	0.1	58.66	22.44	77.56	115.96	1.44	1.17
	0.15	77.25	22.99	87.14	131.65	1.45	1.21

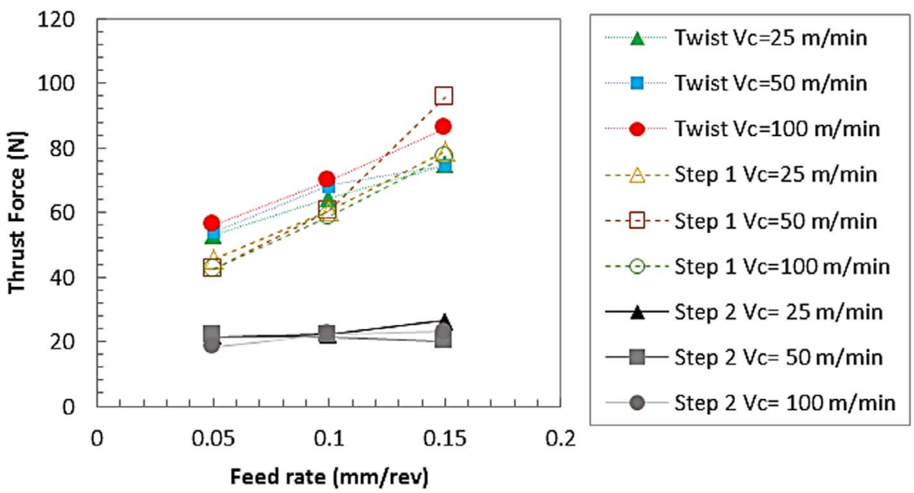

Fig. 3. Evolution of maximum values of thrust force with feed rate for different values of cutting speed.

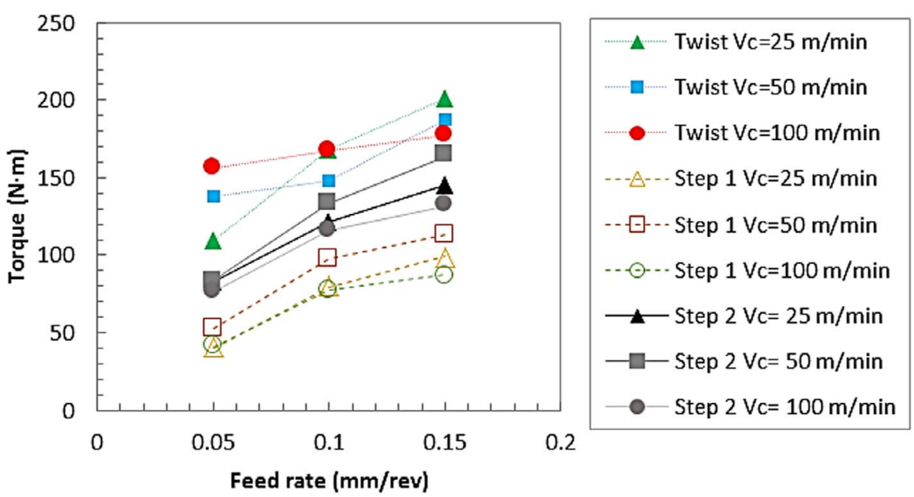

Fig. 4. Evolution of torque with feed rate for different cutting speed.

the base except for the zone inside a circumference with 10 mm diameter that remained free (Fig. 6B). This boundary condition reproduces the effect of the supporting back plate used in the experiments.

The drill was assumed to be rigid. Each ply was modeled using two element types. In the zone around the tool solid elements C3D6R (wedge elements) with six nodes were used in order to minimize the dependence of the results with mesh orientation in the laminate plane. Just one element is located along the ply thickness. The minimum element size was 0.2 mm close to the cutting zone. In the zone far from to the drill entrance, hexagonal elements C3D8R with 8 nodes and reduced integration were chosen with minimum element size around 1 mm (Fig. 6B).

Delamination was modeled using cohesive elements. Meshing strategy for the cohesive plies located in the interface between two CFRP plies was the same as mentioned previously. In this case, the thickness was established equal to 5 µm (see Fig. 7).

4.2. Materials behavior

The chip formation required the implementation of material failure and element erosion criteria. Mechanical behavior of the composite was modeled with the properties detailed in Table 1. The material model used for the carbon/epoxy woven laminate derives from the Chang–-Chang model [52], which has been used in other works of the literature [53,54].

The material model was defined through a VUMAT subroutine. The

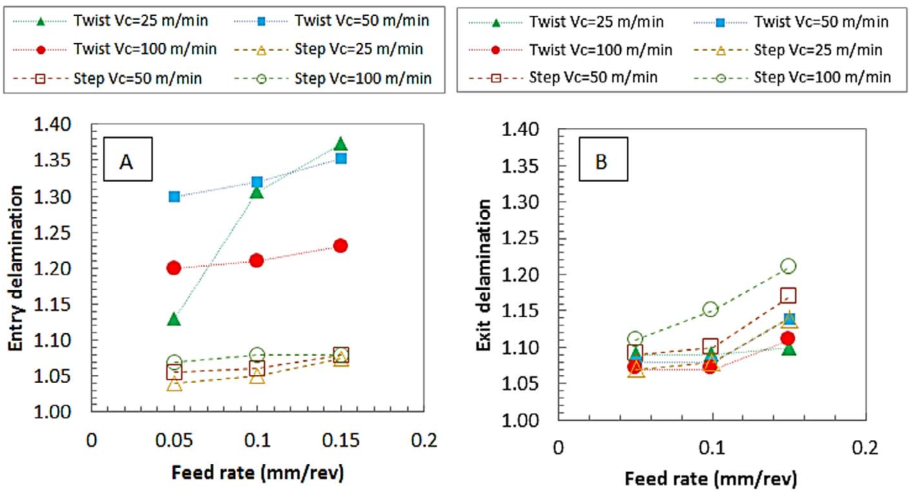

Fig. 5. Evolution of torque with feed rate for different cutting speeds.

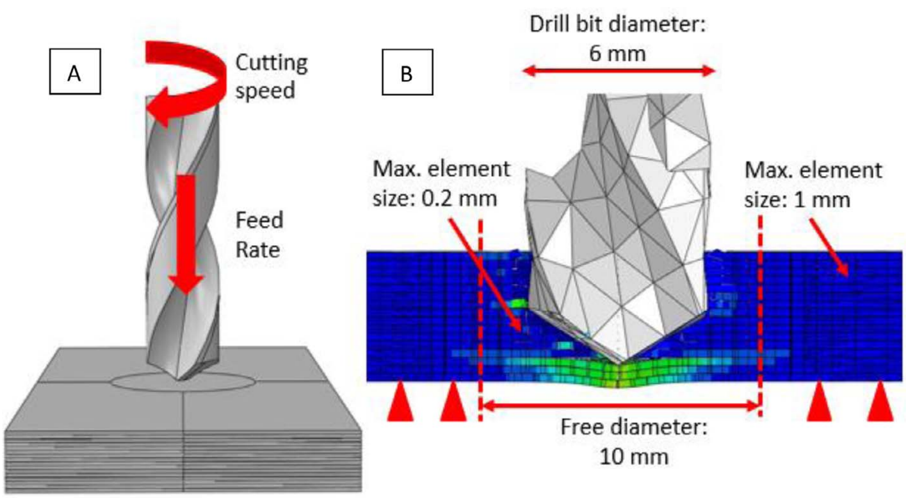

Fig. 6. Movements imposed in the drill (A). Vertical section of the tool penetrating the workpiece showed details of boundary conditions and element size (B).

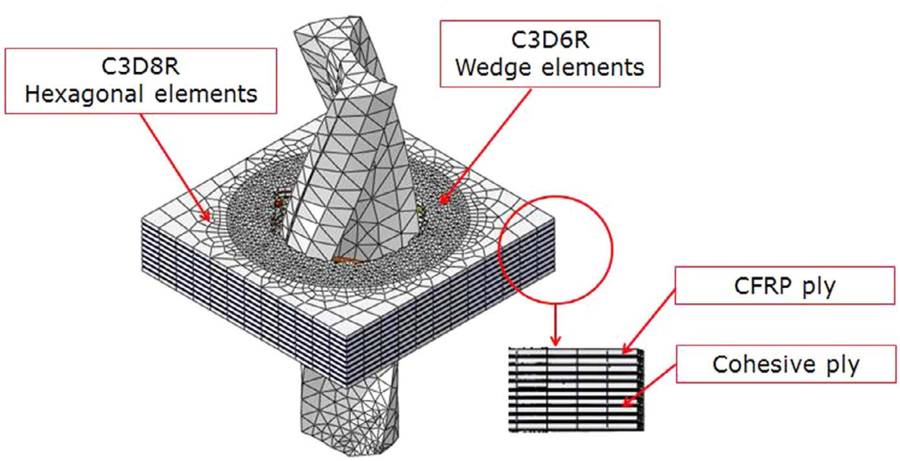

Fig. 7. Scheme of drill step and CFRP modeled with two types of plies, CFRP and cohesive allowing delamination damage prediction.

expressions (1 −4) used to define failure in the composite are presented in Table 5 corresponding to the model defined by López-Puente et al. in [55] and used in several works dealing with dynamic processes on woven CFRPs [50,56]. This model considers four different failure modes: fibre failure at tension and compression in direction 1, fibre failure at tension and compression in direction 2, crushing matrix in plane and crushing matrix through thickness. In Table 5 d_{ij} are the damage variables ranging from 0 to 1, σ_{ij} are the components of the stress tensor, X_t and X_c are the strengths of the laminate in tension and compression for the warp direction, and Y_t and Y_c are the strengths in tension and compression for the fill direction. S_{12}, S_{13} and S_{23} are the shear strengths in the three different planes and Z_c is the strength in the through-thickness direction under compression. When d_{ij} reaches the value 1, the material is completely damaged and strength is lost, thus some of the stress components are set to zero. The strain tensor is calculated after each time increment, and when one of the components reaches the critical value, the element is removed.

Cohesive elements were used to estimate delamination (inter-

Table 5
Failure criteria implemented in the model [55].

Failure mode	Equation
Fibre failure at tension and compression in direction 1	$d_{f1}\begin{cases}\frac{\sigma_{11}}{X_t} & if \quad \sigma_{11} > 0\\ \frac{\lvert\sigma_{11}\rvert}{X_c} & if \quad \sigma_{11} < 0\end{cases}$ (1)
Fibre failure at tension and compression in direction 2	$d_{f2}\begin{cases}\frac{\sigma_{22}}{Y} & if \quad \sigma_{22} > 0\\ \frac{\lvert\sigma_{22}\rvert}{Y_c} & if \quad \sigma_{22} < 0\end{cases}$ (2)
Crushing matrix in plane	$d_{m12} = \left\lvert\frac{\sigma_{12}}{S_{12}}\right\rvert$ (3)
Crushing matrix through thickness	$d_{m3} = \frac{1}{4}\left(\frac{\sigma_{33}}{Z_X}\right)^2 + \frac{Z_C\cdot\sigma_{33}}{4S_{13}S_{23}} + \left\lvert\frac{\sigma_{33}}{Z_C}\right\rvert + max\left[\left(\frac{\sigma_{13}}{S_{13}}\right)^2, \left(\frac{\sigma_{23}}{S_{23}}\right)^2\right]$ (4)

Table 6
Cohesive interface parameters [56].

K_n	$K_{ss} = K_{nn}$	G_n	$G_s = G_t$	t_n	$t_s = t_t$
2 GPa/mm	1.5 GPa/mm	0.6 J/m^2	1.8 J/m^2	11 MPa	45 MPa

laminar damage) based on a traction–separation law. The linear elastic behavior was defined in terms of cohesive interfacial parameters (stiffness and critical energies) presented in Table 6 [56].

The damage initiation is implemented by a quadratic nominal stress criterion given in Eq. (5), where t_n, t_s and t_t are the strengths of the cohesive interface in the normal and in shear directions respectively.

$$\left(\frac{\sigma_{33}}{t_n}\right)^2 + \left(\frac{\sigma_s}{t_s}\right)^2 + \left(\frac{\sigma_t}{t_t}\right)^2 \geqslant 1 \tag{1}$$

Damage evolution criteria in Eq. (6) is characterized by the released rate energy in the three aforementioned directions G_n, G_s and G_t (where $\alpha = 1$). The critical values of the released rate energy are represented as G_n^C, G_s^C and G_t^C.

$$\left(\frac{G_n}{G_n^C}\right)^\alpha + \left(\frac{G_s}{G_s^C}\right)^\alpha + \left(\frac{G_t}{G_t^C}\right)^\alpha \geqslant 1 \tag{2}$$

4.3. Model validation

The model was validated through the comparison to experimental drilling tests. Fig. 8A compares the thrust force evolution for both experimental and numerical cases for cutting speed 100 m/min and feed rate 0.10 mm/rev. The model was validated in terms of maximum thrust force for both steps of the drill bit. The curves show good prediction in terms of magnitude and shape. Fig. 8B represents the maximum values of force for the first section of the drill bit (F_1) and for the second section (F_2). The maximum error is estimated about 11% for this parameter.

The values of the predicted and measured exit delamination factor are shown in Fig. 8C being the maximum error about 3.5%. This error is acceptable for complex machining models. The slightly overestimation of delamination can be explained because of the characterization of the interface with cohesive elements. The properties required for these elements do not account for strain rate dependence, but actually, the response of the interface between plies could be influenced by the rate of the deformation.

The model is assumed to give reasonably predictions, thus it is used to develop a parametrical study.

5. Parametrical study

Once the model was validated, simulations were carried out in order to analyze the influence of cutting parameters, supporting plate and laminate thickness has been studied for the step geometry.

5.1. Cutting parameters

Fig. 9 presents the evolution of thrust force with feed rate for different cutting speeds. It is clear that the influence of feed rate is more significant than the influence of cutting speed. Thrust force increases by 3.8 when the feed rate is multiplied by 4 for constant cutting speed, but

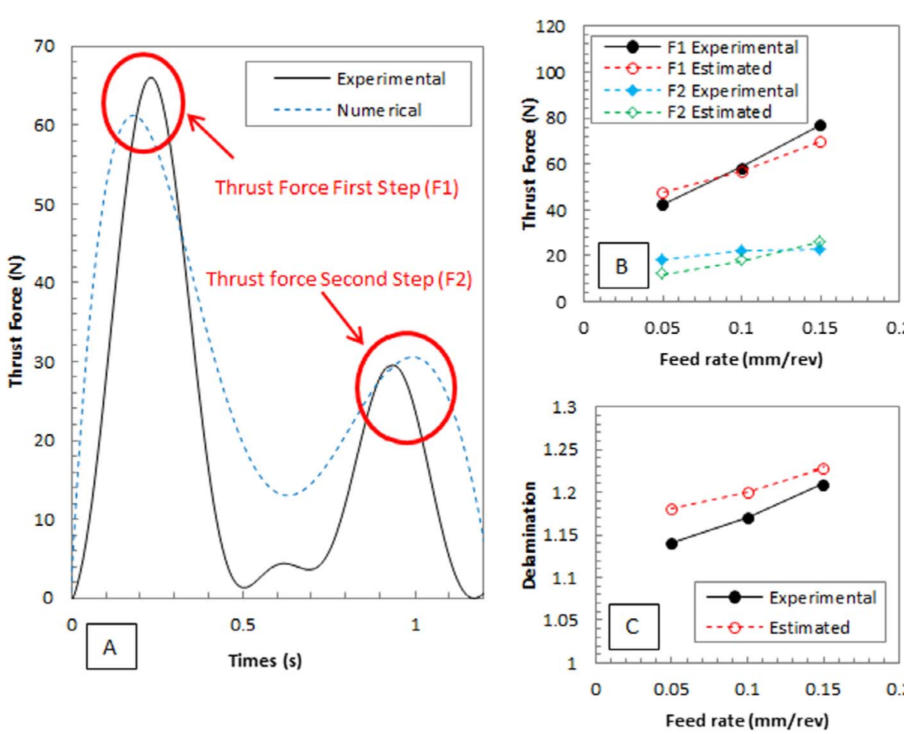

Fig. 8. Comparison of experimental and estimated curves (A), thrust force validation (B) and delamination validation (C).

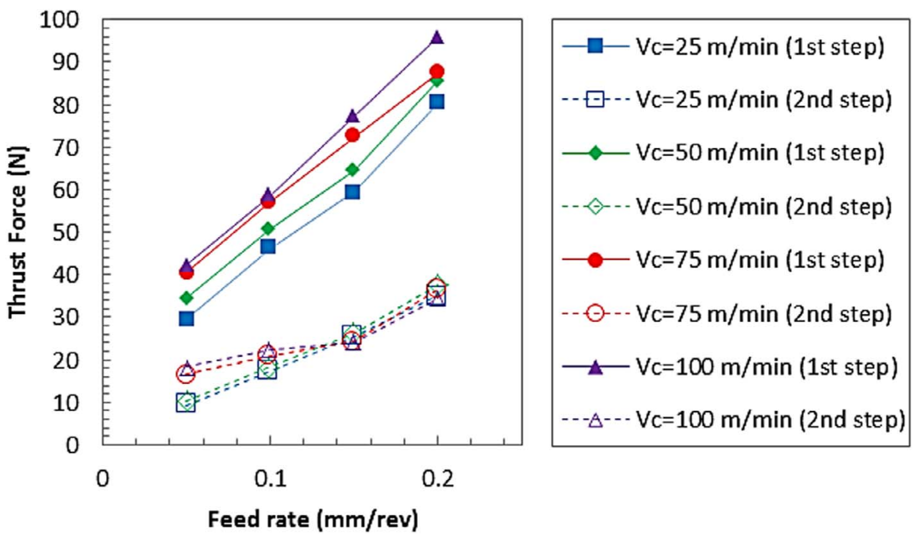

Fig. 9. Variation of maximum thrust force with feed rate for different cutting speeds.

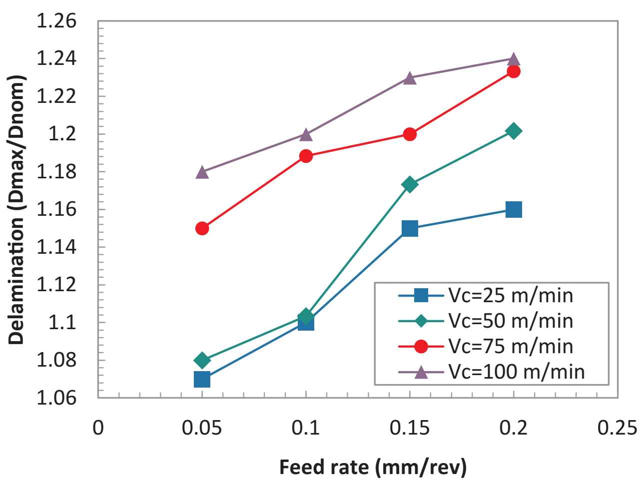

Fig. 10. Evolution of delamination with feed rate speed for different cutting speeds.

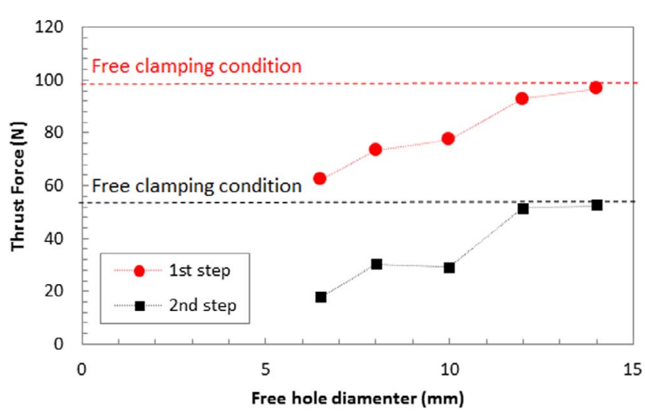

Fig. 11. Evolution of thrust force when increases the free diameter.

it change only 1.9 when the cutting speed is multiplied by 4 (for feed rate constant). However, both parameters present influence on thrust force and delamination, being enhanced when these parameters increase.

Concerning delamination it is observed in Fig. 10. Multiplying the feed rate or the cutting speed by 4 damage factor is multiplied by around 1.1 for both cases.

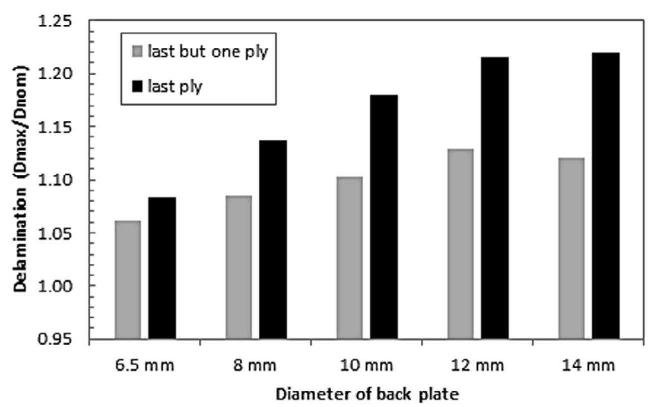

Fig. 12. Influence of the free diameter of back supporting plate in delamination.

5.2. Supporting plate

The influence of the supporting plate diameter was analyzed in Figs. 11 and 12 showing the evolution for thrust force and delamination. In the first graph it can be observed that the increment of the free diameter of the backing support plate results in thrust force increment during drilling, for both sections of the step drill bit. Increasing the clamping diameter from 6.5 to 14 mm, the thrust force increases about 55% for the first section and 193% for the second section. The effect of clamping can be considered negligible for values of the free area higher than 15 mm and equivalent to free surface. Fig. 12 presents the evolution of delamination for the last ply and the adjacent ply. The increments of the damage factor with the variation of the hole of the supporting plate are 13% and 7% respectively for both plies considered.

5.3. Laminate thickness

The thickness of the laminate also influences the thrust force as can be seen in the Fig. 13, different thicknesses were simulated. Results show the influence of the number of layers in the thrust force (A) and delamination (B): both parameters increase with the thickness.

6. Mechanistic model

The numerical results obtained from the simulations allowed the adjustment of a mechanistic model relating force to feed rate and cutting speed for the step geometry (see Table 7). A 3D surface prediction was generated as a function of cutting parameters (feed rate and cutting

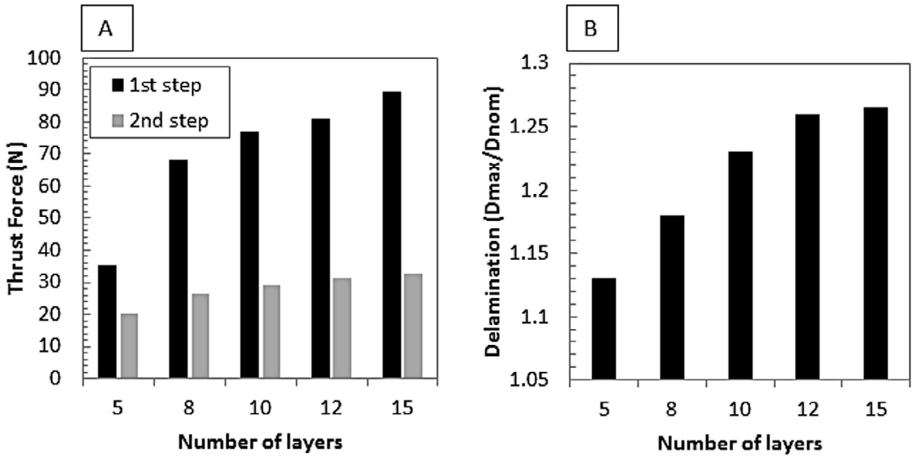

Fig. 13. Influence of the free diameter of back supporting plate in delamination.

Table 7
Prediction equations for step geometry where f is feed rate and V is cutting speed.

Equation	R^2
Force step 1 = $10.60875 + 265.35 * f + 0.213494 * V + 0.210592 * f * V + 224.2 * f^2 - 0.0003388 * V^2$	0.99
Force step 2 = $80.73062 + 90.94 * f + 0.22942 * V - 1.04928 * f * V + 473.6 * f^2 - 4.46e-4 * V^2$	0.97
Delamination = $1.00687 + 0.66167 * f + 1.23e-3 * V$	0.93

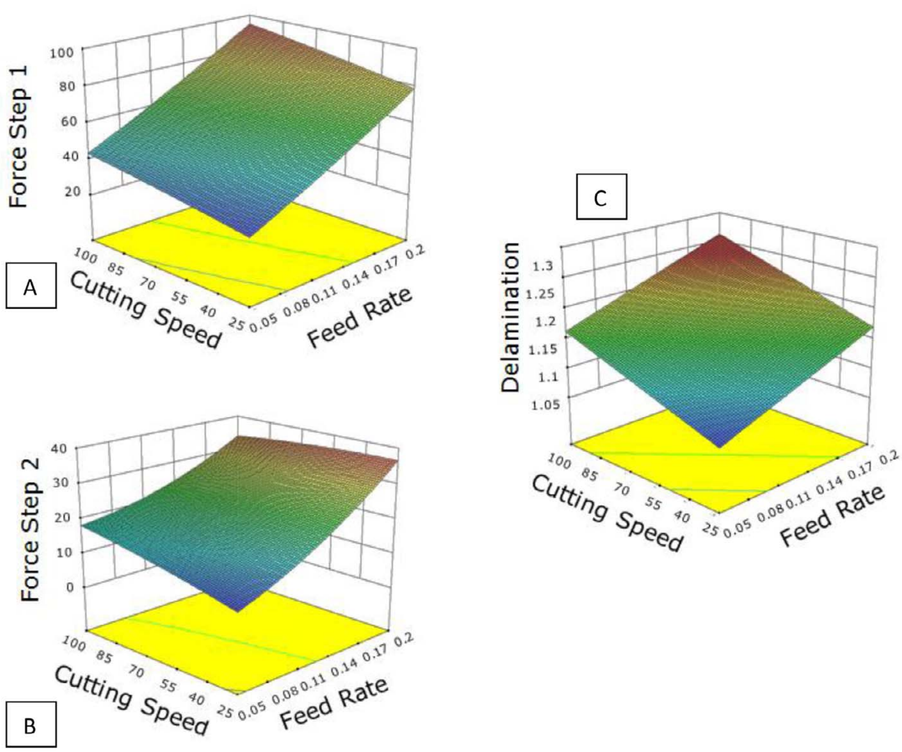

Fig. 14. Prediction surface for thrust force of the first step (A), second step (B) and delamination (C).

speed) able to graphically estimate the values and evolution of the force when the cutting parameters changes as can be seen in Fig. 14 A and B.

The mechanistic model for delamination is presented also in Table 7 with the force equations. The surface prediction is shown in Fig.14C, it can be seen that the influence of the cutting speed is more relevant than thrust force.

7. Conclusions

In this paper an experimental and numerical analysis of CFRPs drilling with stepped drill geometry was developed. The numerical model was validated comparing to experimental results for stepped geometry. Good accuracy was observed when predicting thrust force and delamination factor.

The comparison between stepped drill and twist drill showed lower values of thrust force and delamination factor for the former geometry especially at low feed rates.

A parametrical analysis was carried out using the validated numerical model. The effect of cutting parameters was analyzed finding that increasing both cutting speed and feed rate results in enhanced thrust force and damage factor. Also the effect of using a supporting back plate was checked concluding that its use decreases the damage and improves the quality surface of the drilled hole. Moreover mechanistic models have been adjusted using numerical results, with the goal of obtaining a rapid estimation of delamination factor and thrust force. Surface diagrams were obtained being a simulation tool suitable for industrial applications.

Acknowledgements

The authors acknowledge the financial support for this work from the Ministry of Economy and Competitiveness of Spain under the project DPI2011-25999, FEDER program, and the FPI subprogram associated to the project previously mentioned with the reference BES-2012-055162.

References

[1] Davim JP. Machinability of Fibre-Reinforced Plastics. de Gruyter, 2015 (ISBN: 978-3-11-029225-1).
[2] Voisey KT, Fouquet S, Roy D, Clyne TW. Fiber swelling during laser drilling of carbon fiber composites. Opt Laser Technol 2006;44:1185–97.
[3] Herzog D, Jaeschke P, Meier O, Haferkamp H. Investigations on the thermal effect caused by laser cutting with respect to static strength of CFRP. Int J Mach Tools Manuf 2008;48:1464–73.
[4] Azmir MA, Ahsan AK. A study of abrasive water jet machining process on glass/epoxy composite laminate. J Mater Process Tech 2009;209:6168–73.
[5] Shanmugam D, Nguyen T, Wang J. A study of delamination on graphite/epoxy composites in abrasive waterjet machining. Compos A 2008;39:923–9.
[6] López de Lacalle LN, Fernández A, Olvera D, Lamikiz A, Olvera D, Rodríguez C, et al. Monitoring deep twist drilling for a rapid manufacturing of light highstrength parts. Mech Syst Sig Process 2011;25:2745–52.
[7] Pujana J, Rivero A, Celaya A, López de Lacalle LN. Analysis of ultrasonic-assisted drilling of Ti6Al4V. Int J Mach Tools Manuf 2009;49:500–8.
[8] Haddad M, Zitoune R, Eyma F, Castanie B. Machinability and surface quality during high speed trimming of multi directional CFRP. Int J Mach Mach Mater 2013;13:289–310.
[9] Haddad M, Zitoune R, Bouguerara H, Eyma F, Castanie B. Study of trimming damages of CFRP structures in function of the machining processes and their impact on the mechanical behavior. Compos B 2014;57:136–43.
[10] López de Lacalle LN, Lamikiz A, Campa FJ, Fdz-Valdivielso A. Design and test of a multitooth tool for CFRP milling. J Compos Mater 2009;43(26):3275–90.
[11] Liu DF, Tang YJ, Cong WL. A review of mechanical drilling for composite laminates. Compos Struct 2012;94:1265–79.
[12] Feito N, Díaz-Álvarez J, Díaz-Álvarez A, Cantero JL, Miguélez MH. Experimental analysis of the influence of drill point angle and wear on the drilling of woven CFRPs. Mater 2014;7:4258–71.
[13] Girot F, Iliescu D, Fernandez A, Gutiérrez-Orrantia ME, López de Lacalle LN. Experimental study and modeling of tool wear in drilling and trimming of CFRP. J Compos Adv Mater 2013;23(3):357–85.
[14] Grilo TJ, Paulo RMF, Silva CRM, Davim JP. Experimental delamination analyses of CFRPs using different drill geometries. Compos B 2013;45(1):1344–50.
[15] Davim JP, Reis P. Study of delamination in drilling carbon fiber reinforced plastic (CFRP) using design experiments. Compos Struct 2003;59:481–7.
[16] Gaitonde VN, Karnik SR, Campos Rubio J, Esteves Correia A, Abrao AM, Paulo Davim J. Analysis of parametric influence on delamination in high-speed drilling of carbon fiber reinforced plastic composites. J Mater Process Technol 2008;203:431–8.
[17] Krishnaraj V, Prabukarthi A, Ramanathan A, Elanghovan N, Senthil Kumar M, Zitoune R, et al. Optimization of machining parameters at high speed drilling of carbon fiber reinforced plastic (CFRP) laminates. Compos B 2012;43:1791–9.
[18] Gaugel S, Sripathy P, Haeger A, Meinhard D, Bernthaler T, Lissek F, et al. A comparative study on tool wear and laminate damage in drilling ofcarbon-fiber reinforced polymers (CFRP). Compos Struct 2016;155:173–83.
[19] López de Lacalle LN, Rivero A, Lamikiz A. Mechanistic model for drills with double point-angle edges. Int J Adv Manuf Technol 2009;40:447–57.
[20] Karnik SR, Gaitonde VN, Campos Rubio J, Esteves Correia A, Abrao AM, Davim JP. Delamination analysis in high speed drilling of carbon fiber reinforced plastics (CFRP) using artificial neural network model. Mater Des 2008;29:1768–76.
[21] Tsao CC, Hocheng H. Taguchi analysis of delamination associated with various drill bits in drilling of composite material. Int J Mach Tools Manuf 2004;44:1085–90.
[22] Tsao CC, Hocheng H. Computerized tomography and C-Scan for measuring delamination in the drilling of composite materials using various drills. Int J Mach Tools Manuf 2005;45:1282–7.
[23] Feito N, Diaz-Álvarez A, Cantero JL, Rodríguez-Millán M, Miguélez H. Experimental analysis of special tool geometries when drilling woven and multidirectional CFRPs. J Reinf Plast Compos 2016;35(1):33–55.
[24] Durao P, Goncalves JS, Tavares RS, Albuquerque C, Aguiar A, Torres A. Drilling tool geometry evaluation for reinforced composite laminates. Compos Struct 2010;92:1545–50.
[25] Hocheng H, Tsao CC. Effects of special drill bits on drilling-induced delamination of composite materials. Int J Mach Tools Manuf 2006;46:1403–16.
[26] Hocheng H, Tsao CC. Comprehensive analysis of delamination in drilling of composite materials with various drill bits. J Mater Process Technol 2003;140:335–9.
[27] Shyha IS, Soo SL, Aspinwall D, Bradley S. Effect of laminate configuration and feed rate on cutting performance when drilling holes in carbon fibre reinforced plastic composites. J Mater Process Technol 2010;210:1023–34.
[28] Shyha IS, Aspinwall DK, Soo SL, Bradley S. Drill geometry and operating effects when cutting small diameter holes in CFRP. Int J Mach Tools Manuf 2009;49:1008–14.
[29] Brinksmeier E, Janssen R. Drilling of multi-layer composite materials consisting of carbon fiber reinforced plastics (CFRP), titanium and aluminum alloys. CIRP Ann – Manuf Technol 2002;51:87–90.
[30] Marques T, Durao M, Magalhaes G, Silva F, Tavares RS. Delamination analysis of carbon fibre reinforced laminates: evaluation of a special step drill. Compos Sci Technol 2009;69:2376–82.
[31] Chandrasekharan V, Kapoor SG, Devor RE. A mechanistic model to predict the cutting force system for arbitrary drill point geometry. J Manuf Sci Eng 1998;120:563–70.
[32] Singh I, Bhatnagar N, Viswanath P. Drilling of uni directional glass fiber reinforced plastics: experimental and finite element study. Mater Des 2008;29:546–53.
[33] Khashaba UA, EI-Sobaty IA, EI-Sobaty AI, Megahed AA. Machinability analysis in drilling woven GFR/epoxy composites: part II – effect of drill wear. Compos A 2010;41:1130–7.
[34] Fernandes M, Cook C. Drilling of carbon composites using a one shot drill bit. Part II. Empirical modeling of maximum thrust force. Int J Mach Tools Manuf 2006;46:76–9.
[35] Tsao CC, Hocheng H. Parametric study on thrust force of core drill. J Mater Process Technol 2007;192–193:37–40.
[36] Tsao CC. Prediction of thrust force of step drill in drilling composite materials by Taguchi method and radial basis function network. Int J Adv Manuf Technol 2008;36:11–8.
[37] Upadhyay PC, Lyons JS. On the evaluation of critical thrust for delamination-free drilling of composite laminates. J Reinf Plast Compos. 1999;18:1287–303.
[38] Anand RS, Patra K. Mechanistic cutting force modelling for micro-drilling of CFRP composite laminates. J Manuf Sci Technol 2017;16:55–63.
[39] Olvera D, López de Lacalle LN, Urbikain G, Lamikiz A, Rodal P, Zamakona I. Hole making using ball helical milling on titanium alloys. Mach Sci Technol 2012;16(2):173–88.
[40] Ojo SO, Ismail SO, Paggi M, Dhakal HN. A new analytical critical thrust force model for delamination analysis of laminated composites during drilling operation. Compos B 2017;124:207–17.
[41] Ismail SO, Ojo SO, Dhakal HN. Thermo-mechanical modelling of FRP cross-ply composite laminates drilling: delamination damage analysis. Compos B 2017;108:45–52.
[42] Chinmaya RD, Shin YC. Modeling of machining of composite materials: a review. Int J Mach Tools Manuf 2012;57:102–21.
[43] Santiuste C, Olmedo A, Soldani X, Miguélez MH. Delamination prediction in orthogonal machining of carbon LFRP composites. J Reinf Plast Compos 2012;31(13):875–85.
[44] Abena A, Soo SL, Essa K. Modelling the orthogonal cutting of UD-CFRP composites: development of a novel cohesive zone model. Compos Struct 2017;168:65–83.
[45] Díaz-Álvarez J, Olmedo A, Santiuste C, Miguélez MH. Theoretical estimation of thermal effects in drilling of woven carbon fiber composite. Mater 2014;7:4442–54.
[46] Durao LMP, de Moura MFSF, Marques AT. Numerical simulation of the drilling process on carbon/epoxy composite laminates. Compos A 2006;37:1325–33.
[47] Durao LMP, de Moura MFSF, Marques AT. Numerical prediction of delamination onset in carbon/epoxy composite laminates. Eng Fract Mech 2008;75:2767–78.
[48] Isbilir O, Ghassemieh E. Numerical investigation of the effects of drill geometry on drilling induced delamination of carbon fiber reinforced composites. Compos Struct 2013;105:126–33.
[49] Phadnis VA, Makhdum F, Roy A, Silberschmidt VV. Drilling in carbon/epoxy composites: experimental investigations and finite element implementation. Compos A 2013;47:41–51.
[50] Feito N, Díaz-Álvarez J, López-Puente J, Miguélez MH. Numerical analysis of the influence of tool wear and special cutting geometry when drilling woven CFRPs. Compos Struct 2016;138:285–94.
[51] Feito N, López-Puente J, Santiuste C, Miguélez MH. Numerical prediction of delamination in CFRP drilling. Compos Struct 2014;108:677–83.
[52] Chang F, Chang KA. A progressive damage model for laminated composites containing stress concentrations. J Compos Mater 1987;21:834–55.
[53] Hou JP, Petrinic N, Ruiz C, Hallet SR. Prediction of impact damage in composite plates. Compos Sci Technol 2000;60:273–81.
[54] Iannucci L, Willows M. An energy based damage mechanics approach to modelling impact onto woven composite materials – part I: numerical models. Compos Part A 2003;37(11):2041–56.
[55] López-Puente J, Zaera R, Navarro C. Experimental and numerical analysis of normal and oblique ballistic impacts on thin carbon/epoxy woven laminates. Compos Part A 2008;39:374–87.
[56] Varas D, Artero-Guerrero JA, Pernas-Sánchez J, López-Puente J. Analysis of high velocity impacts of steel cylinders on thin carbon/epoxy woven laminates. Compos Struct 2013;95:623–9.